Discover Applied Sciences

Research

A low-profile antenna with parasitic elements and a DGS-based partial ground plane for 5G/WMAN applications

Liton Chandra Paul[1] · Md. Tanvir Rahman Jim[1] · Tithi Rani[2] · S. M. Muyeen[3] · Muharrem Karaaslan[4] · Sk. A. Shezan[5] · Md. Fatin Ishraque[1] · Volkan Akdogan[4]

Abstract

A low-profile antenna with three parasitic elements is designed and presented for fifth-generation (5G) and wireless metropolitan area network (WMAN) applications. This prototype covers the frequency range of 2.75–4.94 GHz, which is applicable for the lower 5G (3.33–4.2 GHz), WWAN n48 CBRS (US) (3.55–3.7 GHz), WiMAX rel 2 (3.4–3.6 GHz), n77 (3.3–4.2 GHz, most European and Asian countries), n78 (3.3–3.8 GHz, USA), and n79 (4.4–5.0 GHz, China, Hong Kong, Japan, and Russia) bands. The prototype is made of a low-loss, commercially available substrate material known as Rogers RT 5880 ($\varepsilon_r = 2.2$, tan$\delta = 0.0009$) with a thickness of 0.79 mm. The optimized dimension of the proposed antenna is $35 \times 25 \times 0.79$ mm^3 (i.e., 691.25 mm^3). The proposed 10-element array antenna is fed by a 50 Ω feeder. The maximum gain and directivity of the prototype antenna are 4.3 dB and 4.75 dBi, respectively. The radiation efficiency of the prototype varies from 86.79 to 92.14% (simulated) and from 86.23 to 91.48% (measured), and it is 89.48% (simulated) and 90.59% (measured) at 3.225 GHz. The impedance profile of the proposed 10-element array is (49.80-j1.72) Ω, which ensures good impedance matching. The VSWR and surface current of the low-profile antenna are 1.036 and 107.931 A/m at the center frequency of 3.225 GHz, respectively. The value of the scattering parameter (S_{11}) is − 36 dB at the resonant frequency. By using a DGS-based partial ground plane and parasitic elements, it enhances bandwidth to 2.19 GHz. Therefore, the tested prototype is an excellent candidate to be deployed for 5G/WMAN applications with respect to the different presented parametric studies.

Article Highlights

- A low-profile novel antenna prototype with parasitic elements and a defected ground structure (DGS)-based partial ground plane for 5G/WMAN communication has been designed and proposed.
- The prototype of the antenna provides a large bandwidth of 2.75–4.94 GHz which covers the lower 5G (3.33–4.2 GHz), WWAN n48 CBRS (US) (3.55–3.7 GHz), WiMAX rel 2 (3.4–3.6 GHz), n77 (3.3–4.2 GHz, most European and Asian countries), n78 (3.3–3.8 GHz, USA), and n79 (4.4–5.0 GHz, China, Hong Kong, Japan, and Russia) bands.

✉ S. M. Muyeen, sm.muyeen@qu.edu.qa; Liton Chandra Paul, litonpaulete@gmail.com; Md. Tanvir Rahman Jim, tanvirjim017@gmail.com; Tithi Rani, tithi.saha.134040@gmail.com; Muharrem Karaaslan, muharrem.karaaslan@iste.edu.tr; Sk. A. Shezan, shezan.ict@gmail.com; Md. Fatin Ishraque, fatineeruet@gmail.com; Volkan Akdogan, volkan.akdogan@iste.edu.tr | [1]Department of Electrical, Electronic and Communication Engineering, Pabna University of Science and Technology, Pabna 6600, Bangladesh. [2]Department of Electronics and Telecommunication Engineering, Rajshahi University of Engineering and Technology, Rajshahi 6204, Bangladesh. [3]Department of Electrical Engineering, Qatar University, 2713 Doha, Qatar. [4]Department of Electrical and Electronics Engineering, Iskenderun Technical University, Iskenderun, Hatay 31200, Turkey. [5]Department of Electrical Engineering, Engineering Institute of Technology, Melbourne, Australia.

Discover

- The proposed design possesses excellent radiation characteristics and also exhibits very strong agreement between measured and simulated results.
- The design is also validated by both time domain and frequency domain analysis.
- Good gain throughout the large operating band with higher efficiency.

1 Introduction

Nowadays, both software and hardware parts of wireless communication systems for multiple applications are being enriched rapidly. Wideband and ultra-wide band planar microstrip patch antennas have become extremely popular due to their low profile, compactness, low cost, low weight, and simplicity of integration with any wireless device as compared to traditional wire antennas [1, 2]. A 5G communication system is able to provide several significant benefits, like seamless coverage, higher capacity, a higher rate, and lower latency than other previous generations. One promising 5G band for wireless systems has been projected around 3.5 GHz, jointly acknowledged as a sub-6 GHz band or mid-band (under 6 GHz). The mid-band provides a compelling amount of capacity and area coverage [3, 4]. With the demand for high mobility in the modern era, wireless cellular technology has developed step by step, like 1G, 2G, 3G, 4G, and 5G. Currently, researchers are also working on 6G. With the introduction of 5G technology, many smart services, including the Internet of Things (IoT), ultra-reliable low-latency communications (uRLLC), non-orthogonal multiple access (NOMA), massive machine-type communications (mMTC), and enhanced mobile broadband (eMBB) services, were added [5]. In the USA, 3.1–3.55 GHz and 3.7–4.2 GHz, in Europe, 3.4–3.8 GHz, and in China, 3.3–3.6 GHz and 4.8–4.99 GHz bands are regarded as suitable for 5G applications. Table 1 summarizes the spectrum coverage (the key frequency range) for 5G technology.

The multifunctional advantages provided by a smart phone, smart TV, tablet, or laptop are reducing day by day [6–8]. There are a lot of smart and fast services that are possible due to the use of high-speed embedded electronics within the devices [9, 10]. These advantages come from the deployment of compact planar antennas within the handy electronic devices [11, 12]. Some promising antennas are operating within the mid-band 5G, wireless local area network (WLAN) band, or world-wide interoperability for microwave access (WiMAX) applications [13, 14]. The planar antennas are widely deployed in 3G, 4G, 5G, WMAN, wireless fidelity (WiFi), and WiMAX applications for their robustness, light weight, cost effectiveness, dual polarization, support for multiband, and pinpoint management of radiation patterns [15]. Several researchers have proclaimed that an array antenna would be one of the best techniques for improving gain, and it helps to meet the requirement of good impedance matching [16]. In [17], a flexible CPW-fed transparent antenna is developed for sub-6 GHz and WLAN applications by using finite element method (FEM)-based HFSS software. The antenna uses a transparent and flexible PET substrate as well as AgHT-8 conducting material with an electrical size of $0.48\lambda \times 0.64\lambda$. Yerlikaya et al. [18] also designed a compact wideband antenna for sub-6 GHz mobile systems. It has a maximum gain of 2.3 dB, a low bandwidth of 0.8 GHz (3.4–4.2 GHz), and an efficiency of 73%. A FR4 (dielectric constant 4.4)-based $180 \times 60 \times 1.6$ mm^3 dual band antenna had been proposed for LTE-R and 5G communications [19]. The antenna possesses narrow bandwidths (0.13 GHz and 0.5 GHz). The authors in [20] have discussed a WiFi/5G antenna that is made by Rogers RT/Duroid substrate and whose dimension is $46 \times 46 \times 3.175$ mm^3 ($0.37\lambda \times 0.37\lambda$). The bandwidths of the antenna are 0.1 GHz and 0.36 GHz. In [21], a high-volume ($0.57\lambda \times 0.57\lambda$) stacked microstrip antenna working from 3.3 to 3.6 GHz has been designed. The reflection coefficient of the antenna is -18.33 dB at 3.45 GHz. A planar antenna ($40 \times 30 \times 1.6$ mm^3) with a bandwidth of 0.72 GHz and a maximum gain of 2.5 dB has been designed for 5G applications. The antenna resonates at 3.83 GHz, where the reflection coefficient is -31.15 dB [22]. Another FR4-based multi-slotted $32.4 \times 27.9 \times 1.6$ mm^3 planar antenna is introduced in [23]. It possesses a total bandwidth of 0.019 GHz. It also provides a peak gain of 4.2 dB at 3.5 GHz and a reflection coefficient of -26.5 dB. A FR-4 based multiband monopole antenna with a low gain (1.5–2 dB) and efficiency (around 80%) has been designed for futuristic wireless communications [24]. A low-profile and directive metamaterial antenna (60×40 mm^2) for 5G, the Internet of Things (IoT), healthcare systems, and smart homes is composed of Rogers RO4350B, which has a maximum gain of 7.14 dB with good impedance matching and a standard VSWR [25]. Abdulbari et al. designed a Rogers/Duriod 5880 LZ-based T-shaped planar antenna ($22 \times 24 \times 0.25$mm^3) with a fractional bandwidth of 42.81% at 3.6 GHz for 5G applications [26]. Therefore, from the above discussion, it is obvious that there is some room for further improvement of the antenna system for 5G and WMAN applications.

Table 1 Spectrum coverage for 5G technology [5]

Sub-1 GHz	1–6 GHz	Above 6 GHz
Coverage layer	Coverage and capacity layer	super data layer
Wide area and deep indoor coverage mMTC, eMBB, uRLLC	mMMTC (no deep coverage), eMBB, uRLLC	Supports high data rates eMBB, uRLLC

The prime aim of this work is to enhance bandwidth, gain, and efficiency with a compact volume. Two branches of hexagonal elements and three parasitic elements are introduced in the design to achieve the goal. At first, the design and optimization steps have been accomplished by using the CST-MWS suite, and then fabrication and measurement have been done in microwave laboratory. The information flow of the article is presented as follows: The design structure, fabricated prototype, and equivalent circuit of the hexagonal array antenna are described in Sect. 2. Then, the corresponding results, different parametric studies and analyses, as well as compatibility with some relevant works, are incorporated in Sect. 3. Finally, key findings and concluding remarks from the studies are presented in Sect. 4.

2 Design structure and evolution process

This section describes the designed structure and evolution steps of the proposed low-profile 10-hexagonal element array antenna with three parasitic elements and a DGS-based partial ground plane for 5G/WMAN applications. Among the three parasitic elements, two are placed on both sides of the main feeder, and one is placed at the top of the partial ground plane. A H-shaped slot is introduced in the partial ground plane. Figure 1a–c show the evolution process of the designed antenna, amplified hexagonal element, and fabricated prototype, respectively. Initially, two hexagonal elements are used and the performance is analyzed. Then, two elements have been added at every step for further improvement of the antenna's performance. Finally, the proposed antenna has 10 elements in total, which provides the best performance for the intended applications. A comparably lower-lossy dielectric material, Rogers RT5880 (2.2, 0.0009) with a thickness of 0.79 mm, is used for the design. The ground plane is made of copper (annealed) with a thickness of 0.035 mm. Initially, the dimensions of the design are estimated by the following formulas with equation numbers (1–4), then optimized to a suitable value [27]. The patch width (W) of the proposed antenna is determined by:

Patch width,

$$W_p = \frac{c}{2f_r}\sqrt{\frac{2}{\varepsilon_r + 1}} \tag{1}$$

where c = Velocity of light, f_r = Resonance frequency and ε_r = Dielectric constant length,

$$L = 0.412h \frac{\left(\varepsilon_{reff} + 0.3\right)\left(\frac{W_P}{h} + 0.264\right)}{\left(\varepsilon_{reff} - 0.258\right)\left(\frac{W_P}{h} + 0.8\right)} \tag{2}$$

Antenna is prone to the fringing effect, which makes the antenna's patch appear electrically larger than its actual size. It is important to note that an increase in substrate height speeds up fringing and causes the feedline and resonance frequency to be farther apart.
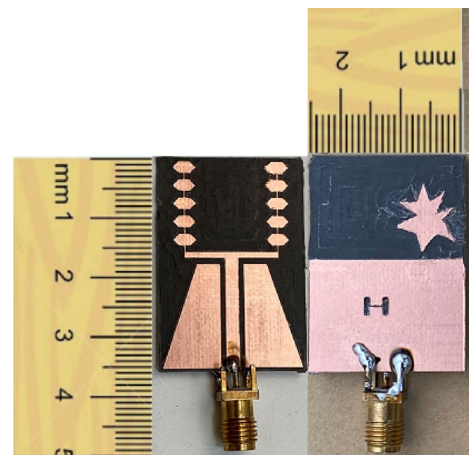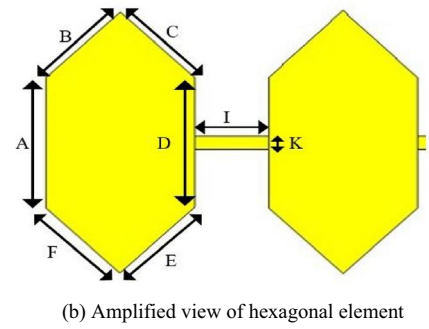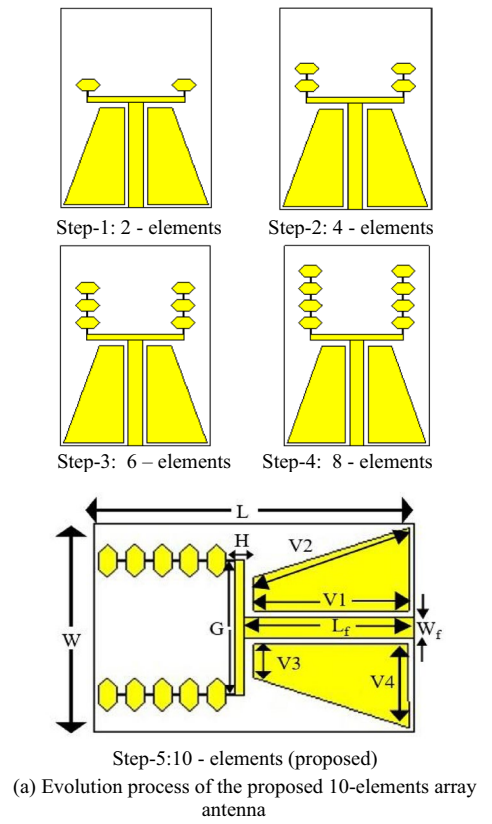
Effective length,

$$L_{eff} = \frac{c}{2f_r\sqrt{\varepsilon_{reff}}} \tag{3}$$

and Patch length,

$$L_p = L_{eff} - 2\Delta L \tag{4}$$

Fig. 1 Proposed low-profile proposed 10-elements array antenna

Step-1: 2 - elements

Step-2: 4 - elements

Step-3: 6 – elements

Step-4: 8 - elements

Step-5:10 - elements (proposed)

(a) Evolution process of the proposed 10-elements array antenna

(b) Amplified view of hexagonal element

(c) Fabricated prototype

Finally, the optimized volume of the low-profile hexagonal element array antenna is 35 mm × 25 mm × 0.79 mm. The antenna model contains 10 hexagonal patch elements, which are connected to two parallel branches. The length (G) and width (H) of the connecting strip of two branches are 16.2 mm and 1 mm, respectively. The feeder length (L_f) is 18.5 mm, and the feeder width (W_f) is 2.4 mm. The lengths of the four arms of trapezoid parasitic elements are 17 mm, 18.03 mm, 4 mm, and 10 mm, which are denoted as V1, V2, V3, and V4, respectively. A 50 Ω microstrip feedline technique is used to energize the proposed hexagonal element partial grounded array antenna.

From the amplified view of the hexagonal element as shown in Fig. 1b, the patch of 10-element array antenna is an irregular hexagon having six arms: A = 2 mm, B = 1.41 mm, C = 1.41 mm, D = 2 mm, E = 1.41 mm, and F = 1.41 mm. The length of the connecting strip of two successive hexagonal elements (I) is 1 mm, while the width of the connecting strip of two successive hexagonal elements (K) is 0.2 mm. The list of optimized parameters for the low-profile MPA is summarized in Table 2. The area of the ground plane is 18.5 × 25 mm². In this research work, waveguide port excitation k = 8.55 is used during port creation, and the line impedance is adjusted to 50 Ώ. The estimated range of the excitation coefficient (k) is 4.64–8.68. The DGS-based ground plane is not only used to widen bandwidth but also to reduce antenna volume. Figure 2 shows an equivalent circuit diagram of the proposed antenna. A parallel combination of R_1, C_1, and L_1 is replicated by the antenna's main feeder. Two trapezoid parasitic elements produce R_2, C_2, L_2 and R_3, C_3, L_3. The gaps between main feeder and trapezoid parasitic elements are represented by C_4 and C_5, respectively. Each hexagonal patch element of the proposed antenna is represented individually by a resistor (R_4–R_{13}), an inductor (L_5–L_{14}) and a capacitor (C_8–C_{17}). The gaps between sub-feeder and trapezoid parasitic elements are C_6 and C_7.

3 Results and analysis

Firstly, the design and optimization of the 10-hexagonal element array antenna have been accomplished by using a licensed CST-MWS suite. Thereafter, it is fabricated and measured in our microwave laboratory. The simulated and measured reflection coefficient curve of the low-profile 10-element array antenna is depicted in Fig. 3. It shows that the center frequency is 3.225 GHz and its working frequency range is 2.75–4.94 GHz. The 10-element array antenna has a good reflection coefficient of − 36 dB at 3.225 GHz and a wide bandwidth of 2.19 GHz. The designed low-profile array antenna covers the lower 5G (3.33–4.2 GHz), WWAN n48 CBRS (US) (3.55–3.7 GHz), WiMAX rel 2 (3.4–3.6 GHz), n77 (3.3–4.2 GHz,

Table 2 Geometrical parameters

Description	Symbol	Value (mm)
Ground layer length	Lg	18
Length of arm of H slot	m	3
Width of arm of H slot	n	1
Length of connecting arm of H slot	p	2
Width of connecting arm of H slot	q	0.5
Length of 1st arm of hexagonal element	A	2
Length of 2nd arm of hexagonal element	B	1.41
Length of 3rd arm of hexagonal element	C	1.41
Length of 4th arm of hexagonal element	D	2
Length of 5th arm of hexagonal element	E	1.41
Length of 6th arm of hexagonal element	F	1.41
Length of connecting strip of two successive hexagonal element	I	1
Width of connecting strip of two successive hexagonal element	K	0.2
Length of connecting strip of two branches	G	16.2
Width of connecting strip of two branches	H	1
Feeder length	L_f	18.5
Feeder width	W_f	2.4
Length of 1st arm of trapezoid parasitic element	V1	17
Length of 2nd arm of trapezoid parasitic element	V2	18.03
Length of 3rd arm of trapezoid parasitic element	V3	4
Length of 4th arm of trapezoid parasitic element	V4	10

Fig. 2 Equivalent circuit of the antenna
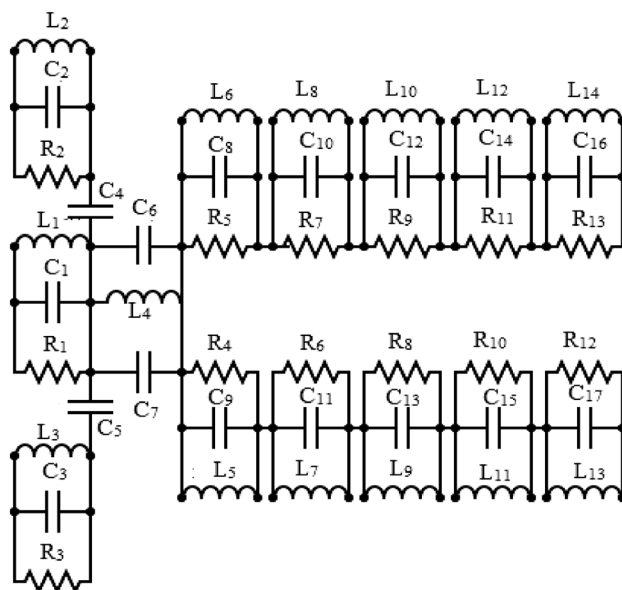
most European and Asian countries), n78 (3.3–3.8 GHz, USA), and n79 (4.4–5.0 GHz, China, Hong Kong, Japan, and Russia) bands. The S11 measurement setup at the microwave laboratory is presented in Fig. 4.

The equivalent circuit of the proposed antenna has been designed, optimized, and simulated by advanced design system (ADS) software. The reflection coefficient of the low-profile proposed 10-element array antenna and the response of its equivalent circuit have been compared in Fig. 5. From the comparison, it is obvious that both responses agree with each other. All the resistors, capacitors, and inductors have been adjusted to suitable values to get a similar response. The reflection coefficient and gain responses of the antenna during all five steps of the evolution process are recorded and presented in Figs. 6 and 7, respectively. By increasing the number of hexagonal elements in the array, the return loss reduces and the gain increases. In the case of 10-hexagonal elements, the resonant frequency is shifted to the left side, and it shows enhanced gain compared to the 8-element array antenna, which makes the antenna more suitable for our aforementioned intended wireless applications. The proposed 10-element antenna shows the best gain profile of all other evolution steps.

The impact of the largest parallel arms, A and D, on the reflection coefficient of the proposed low-profile 10-element array antenna is illustrated in Fig. 8. It is clear to see that the operating frequency band is most suitable for the length of A = D = 2 mm. With an increase in the weights of A and D, the bandwidth becomes narrower, and at the same time, it increases the return loss. The antenna bandwidth increases, but the resonant frequency shifts to the higher frequency,

Fig. 3 Reflection coefficient of the 10-elements array antenna
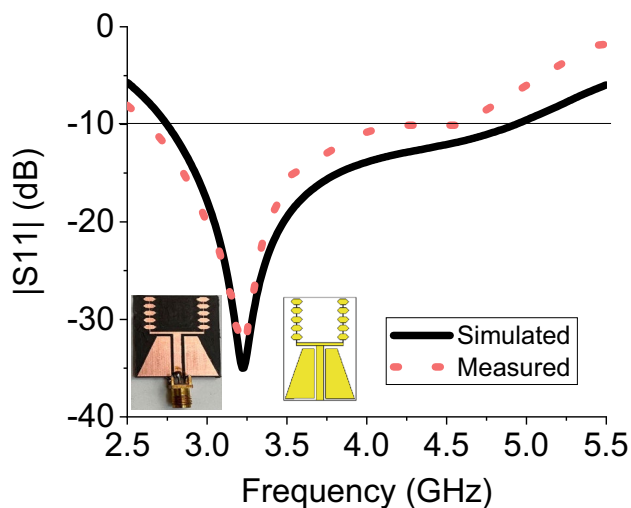
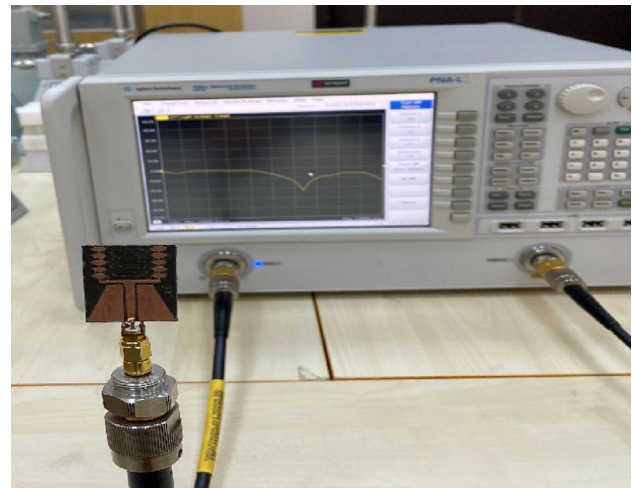**Fig. 4** |S$_{11}$| measurement setup at microwave laboratory

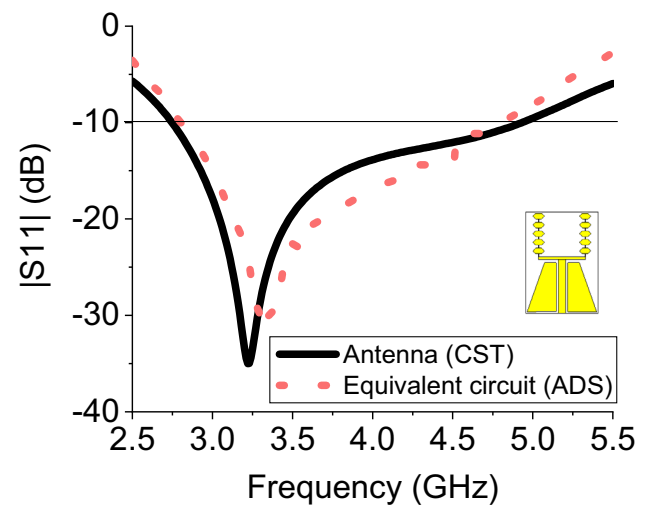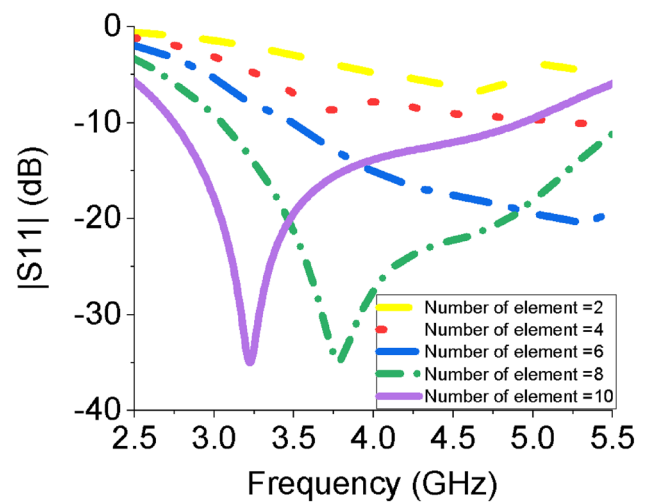**Fig. 5** Reflection coefficient of the antenna and equivalent circuit of the antenna

Fig. 6 Impact of number of elements on reflection coefficient

and return loss increases with increasing both the width of the connecting strip of two successive hexagonal elements (K) and the length of the connecting strip of two branches (G), as presented in Fig. 9. Therefore, K = 0.2 mm and G = 16.2 mm are the best combination for our target applications. Similarly, feedline length and length of the 1st arm of the trapezoid

Fig. 7 Impact of number of elements on gain
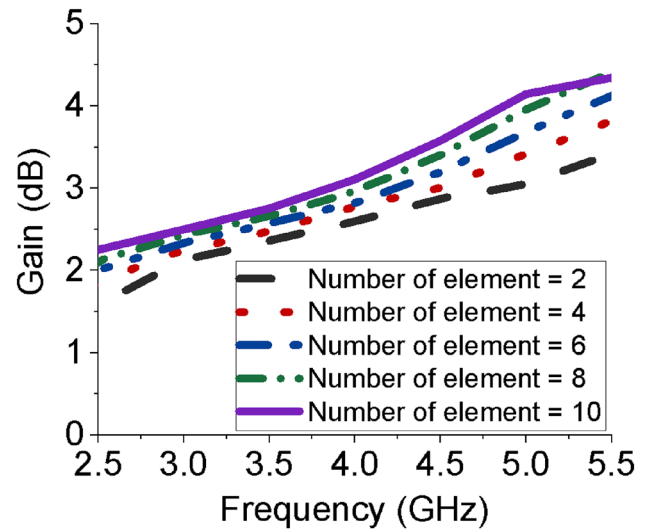
Fig. 8 Impact of A and D on reflection coefficient
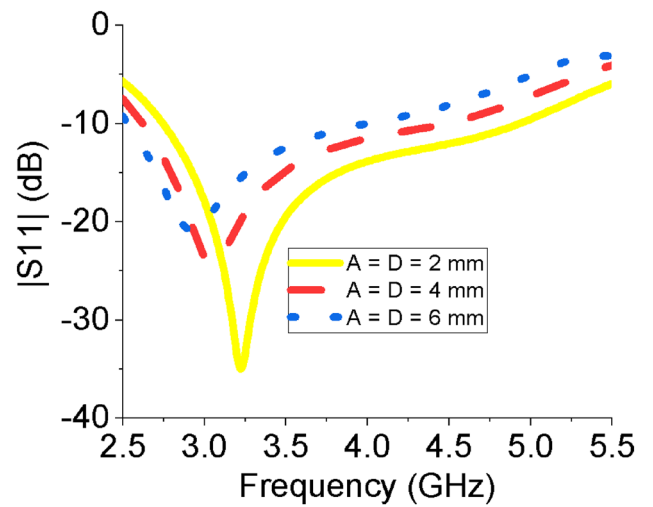
Fig. 9 Impact of K and G on reflection coefficient
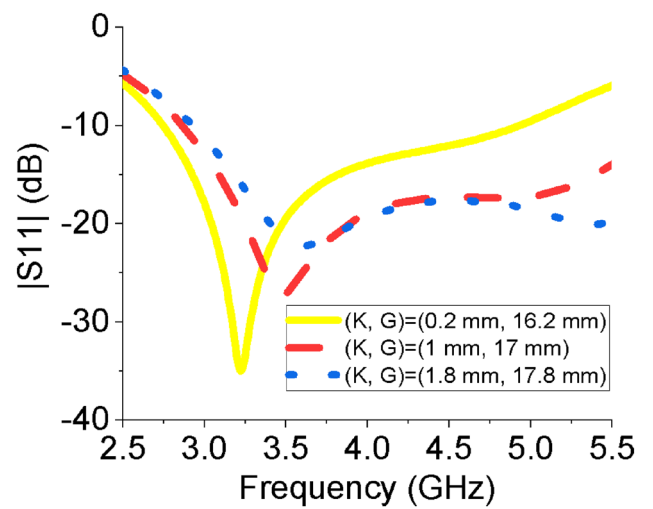
Fig. 10 Impact of Lf and V1 on reflection coefficient
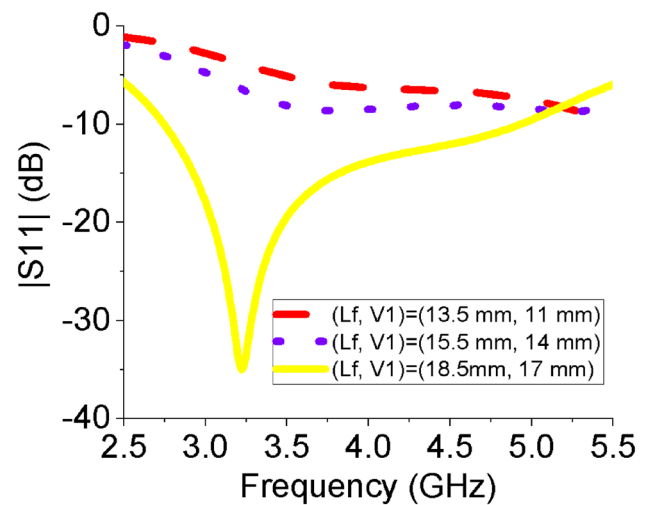
parasitic element have also been studied in Fig. 10. The optimized values are Lf = 18.5 mm and V1 = 17 mm. It also ensures good impedance matching with a reflection coefficient of − 36 dB at 3.225 GHz. A slotted partial ground has been implemented in the proposed 10-element hexagonal patch array antenna, where the area of the partial ground layer is 25 mm × 18 mm. Lg = 18 mm is the best optimized value as presented in Fig. 11. The optimized DGS-based ground plane not only increases the bandwidth but also reduces reflection loss.

The maximum surface current is 107.931 A/m at 3.225 GHz, as presented in Fig. 12. The higher-current conducting regions are the lower part of the main feeder, connecting the strip line of two branches and connecting strips of two successive hexagonal elements. The impedance profile of the proposed 10-element hexagonal patch array antenna is depicted in Fig. 13. The impedance of the antenna is (49.80-j1.72) Ω at 3.225 GHz, which tends to have a pure resistive port impedance of 50 Ω. The gain and directivity of the 10-element array antenna are 2.5 dB and 3.2 dBi at 3.225 GHz, as presented in Fig. 14. The ranges of gain and directivity are 2.3–4.3 dB and 3.1–4.75 dBi, respectively, within the operating frequency of 2.75–4.94 GHz. From the E-field radiation pattern presented in Fig. 15 of the hexagonal patch elements array antenna, the main lobe magnitude is 7.39 V/m for $\phi = 0°$ and 7.31 V/m for $\phi = 90°$, while the main lobe direction is 172° for $\phi = 0°$ and 178° for $\phi = 90°$ at 3.225 GHz. On the other hand, from the H-field pattern presented in Fig. 16 of the low profile array antenna, the main magnitude is 0.0196A/m for $\phi = 0°$ and 0.0194A/m for $\phi = 90°$, whereas the main lobe direction is 172° for $\phi = 0°$ and 178° for $\phi = 90°$. By applying the DGS-based partial ground technique and parasitic elements simultaneously, the side lobe levels are reduced. The 3 dB angular beam width is 84.7° and the side lobe level is − 1.1 dB at $\phi = 0°$ and 3.225 GHz for both fields.

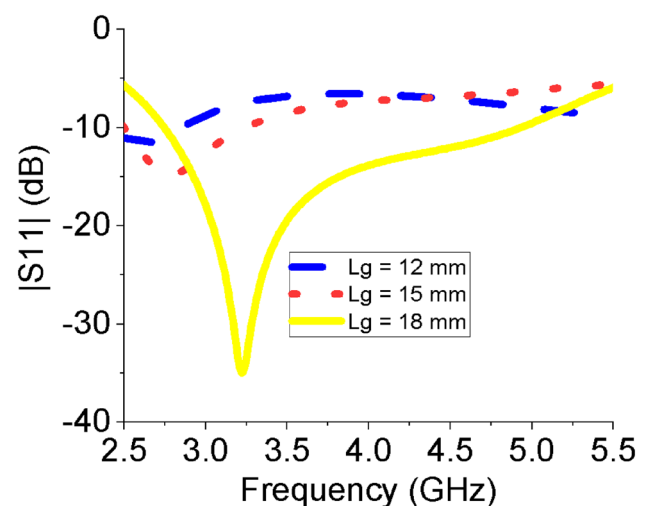**Fig. 11** Impact of Lg on reflection coefficient
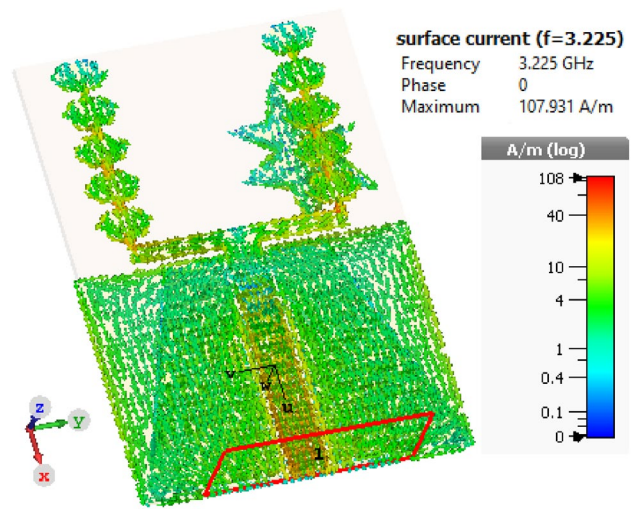
Fig. 12 Current distribution

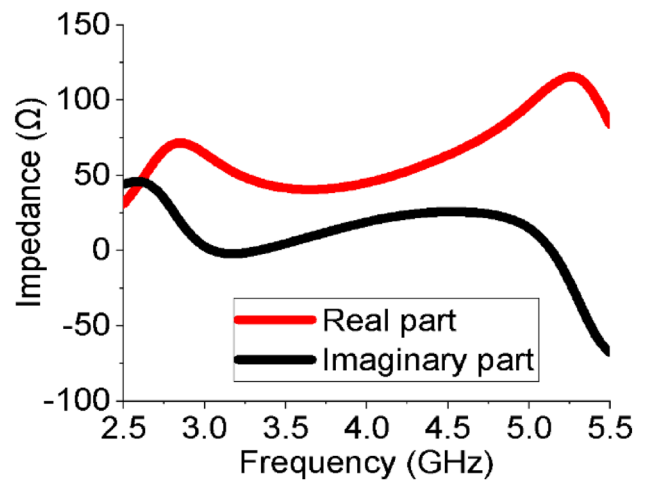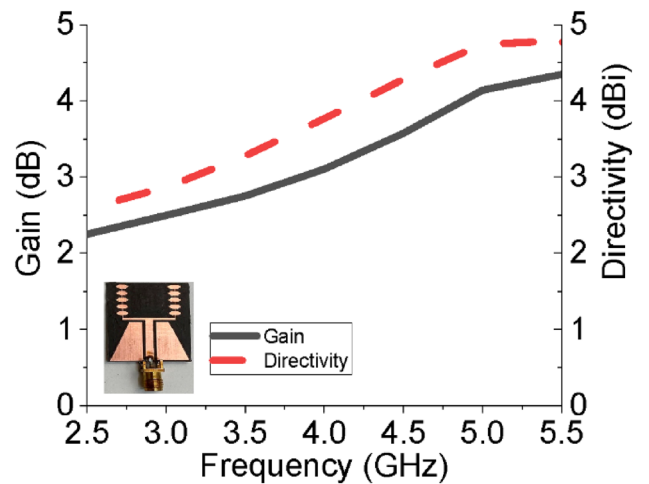**Fig. 13** Impedance of the 10-elements array antenna

Fig. 14 Gain and directivity of the 10-elements array antenna

The radiation efficiency is the ratio of gain to directivity (G/D), i.e., $\eta_{rad} = G(dB) - D(dB)$. Antenna efficiency represents the standard of having the ability to radiate power into free space. Figure 17 depicts the radiation efficiency of the proposed low-profile 10-element hexagonal patch array antenna. The efficiency never drops below 86.23%. It varies from 86.79 to 92.14% (simulated) and from 86.23 to 91.48% (measured), and it is 89.48% (simulated) and 90.59% (measured)

Fig. 15 E-field of the 10-elements array antenna
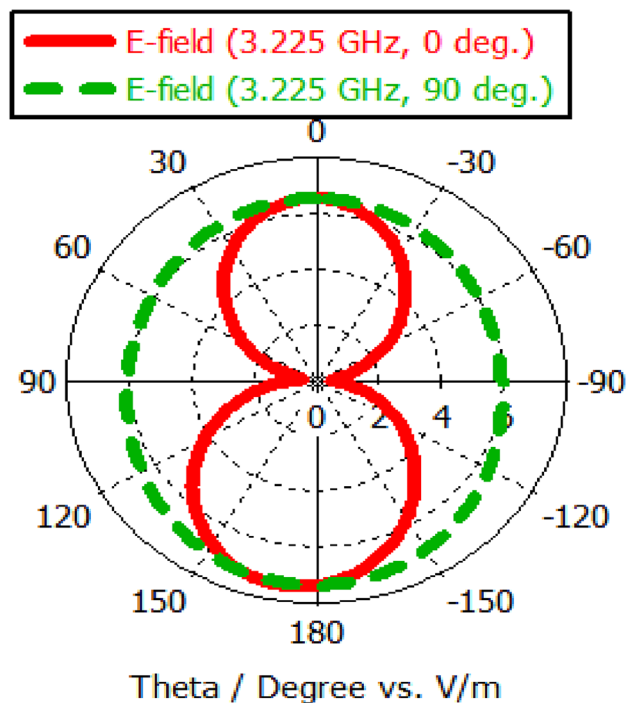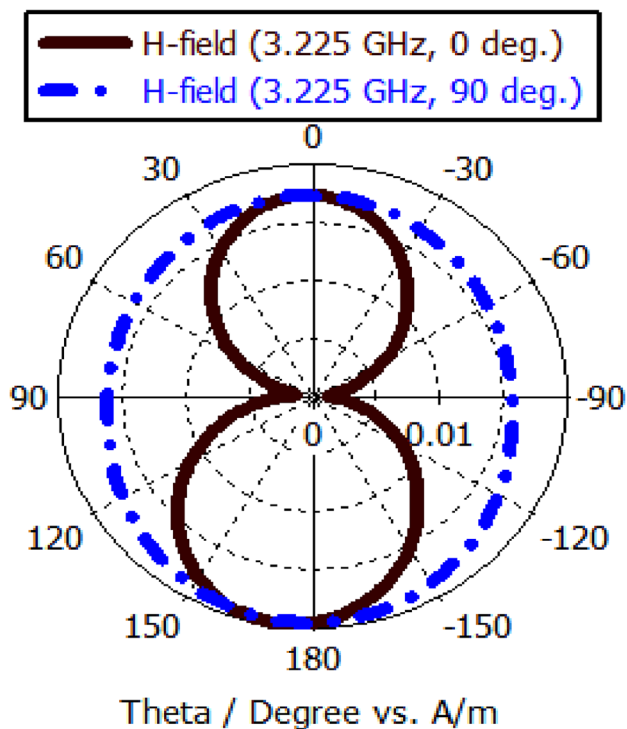

Fig. 16 H fields of the 10-elements array antenna

at 3.225 GHz. The maximum radiation efficiency of the prototype low-profile MPA is 92.14%. The value of the voltage standing wave ratio (VSWR) of a low-profile array antenna is 1.036 at 3.225 GHz, which is close to unity, and 1 < VSWR < 2 within the whole operating band of 2.75–4.94 GHz, as presented in Fig. 18. Therefore, it clarifies good impedance matching because an antenna's impedance matching is essential to transferring maximum power.

A comparison between some relevant recently published works and our presented work is depicted in Table 3. Due to the use of the low-loss dielectric material Rogers RT 5880, which has a thickness of 0.79 mm, the antenna possesses a

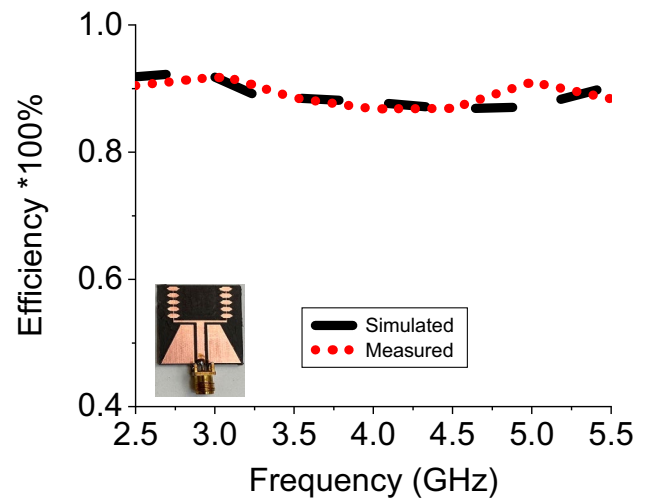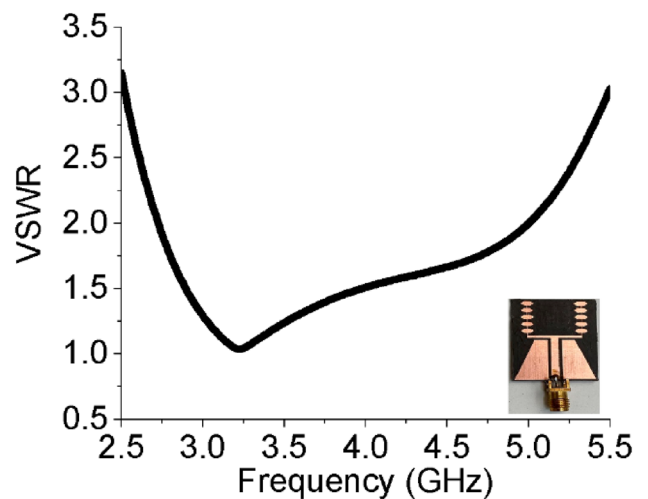**Fig. 17** Efficiency of the 10-elements array antenna

Fig. 18 VSWR of the 10-elements array antenna

higher efficiency of 92.14% with great gain stability within the whole operating frequency range of 2.75–4.94 GHz. The main contribution of this work is the bandwidth and efficiency enhancement of the antenna and keeping the antenna size compact. Though the area of the antenna in [28] is comparatively smaller, its bandwidth and efficiency are too small compared to our proposed 10-element array antenna. The proposed compact 10-element hexagonal patch array antenna provides the highest bandwidth of 2.19 GHz as well as the highest efficiency of 92.14% of all the papers mentioned in the comparison table. It also ensures compactness ($0.32\lambda \times 0.23\lambda$) and a maximum gain of 4.3 dB with a very low VSWR of 1.036. Therefore, the designed low-profile array antenna is more suitable for the intended 5G/WMAN.

4 Conclusion

In this article, a 10-element hexagonal patch compact array antenna (691.25 mm^3) with a H-shaped slotted partial ground plane is designed and tested practically. The obtained outcomes demonstrate the potential of the prototype antenna to comply with 5G/WMAN applications allocated by the Federal Communications Commission (FCC). The − 10 dB bandwidth of the prototype antenna is 2.19 GHz, with a good reflection coefficient of − 36 dB at 3.225 GHz. The VSWR over 2.75–4.94 GHz satisfies 1 < VSWR < 2. The introduction of parasitic elements and the increment of the number of hexagonal patch elements in the array enhance the gain and directivity of the antenna. Other different parametric studies, such as the impact of the length of the largest parallel arms of hexagonal elements, the length of the partial ground, the length of the main feeder, the width of the connecting strip of two successive hexagonal elements, the length of

Table 3 Comparison table

Parameter	Reference no.									This work
	[17]	[18]	[20]	[21]	[22]	[23]	[25]	[28]	[29]	
Size (L×W×h) mm³	58×78×0.9	180×60×1.6	46×46×3.175	52×52	40×30×1.6	32.4×27.9×1.6	60×40×1.52	23×15×1.605	48×35×1.62	35×25×0.79
Electrical size	0.75λ×1.01λ	2.1λ×0.7λ	0.37λ×0.37λ	0.57λ×0.57λ	0.44λ×0.33λ	0.37λ×0.32λ	0.85λ×0.57λ	0.27λ×0.18λ	0.3λ×0.22λ	0.32λ×0.23λ
Dielectric material	PET	FR4	Rogers RT/Duroid	FR4	FR4	FR4	Rogers RO 4350B	FR4	FR4	Rogers RT 5880
Centre frequency (GHz)	5.2	≈ 0.70, ≈ 3.4	2.475, 3.45	3.45	3.83	3.5	4.34	3.72	~ 3.4	3.225
Reflection coefficient (dB)	− 23	≈ − 13, ≈ − 36	~ − 22	− 18.33	− 31.15	− 26.5	− 20	− 35	~ − 29	− 36
Maximum Gain (dB)	3	2.4, 6.1	~ 4	4.46	2.5	4.2	7.14	4.27	4.044	4.3
Coverage range (GHz)	3.89–5.97	0.66–0.79, 3.28–3.78	2.44–2.54, 3.19–3.55	3.3–3.6	3.28–4.0	3.40 − 3.59	4.27−4.4	3.55–4.2	1.85–3.8	2.75−4.94
BW (GHz)	2.08	0.13, 0.5	0.1, 0.36	0.3	0.72	0.019	0.13	0.65	1.95	2.19
Maximum Efficiency (%)	80	–	–	–	–	≈82	90	80	92	92.14
Applications	WLAN, Sub-6 GHz	LTE-R, 5G	WiFi, 5G	WiMAX	5G	Sub-6 GHz, WiMAX, LTE	5G, Sub-6 GHz	5G, WiMAX	4G, 5G and NB-IoT	5G, Sub-6 GHz, WMAN, WiMAX, WWAN, LTE

the connecting strip of two branches, the height of trapezoidal parasites, etc., have been studied in detail. Due to the properties of huge bandwidth, simplicity, compactness, high gain, massive efficiency, very good extensive parametric studies, and the agreement between simulation and experimental results of the fabricated 10-element antenna prototype, it could be deployed as a good competitor for high-speed 5G/WMAN applications.

Data availability All data generated or analyzed during this study are included in this published article.

Declarations

Competing interests The authors declare no competing interests.

References

1. Kodali RR, Siddaiah P, Giriprasad MN. Arrow cross shape slotted fractal antenna with enhanced bandwidth for Wi-Fi/WiMAX/WLAN application. Prog Electromagn Res C. 2022;119:115–24. https://doi.org/10.2528/PIERC22012708.
2. Abed AT, Singh MSJ, Thiruchelvam V, Duraikannan S, Tawfeeq OA, Tawfeeq BA, Islam MT. Challenges and limits of fractal and slot antennas for WLAN, LTE, ISM, and 5G communication: a review paper. Ann Telecommun. 2021;76:547–57. https://doi.org/10.1007/s12243-020-00828-6.
3. Ahmad I, Khan WUR, Dildar H, Ullah S, Ullah S, Mufti N, Kamal B, Ahmad T, Ghaffar A, Hussien MI. A pentaband compound reconfigurable antenna for 5G and multi-standard sub-6GHz wireless applications. Electronics. 2021;10(20):1–17. https://doi.org/10.3390/electronics10202526.
4. Roy S, Biswas AK, Ghosh S, Chakraborty U, Sarkhel A. Isolation improvement of dual-/quad-element textile MIMO antenna for 5G application. J Electromagne Waves Appl. 2021;35(10):1337–53. https://doi.org/10.1080/09205071.2021.1888808.
5. A White Paper on Enabling 5G in India. 22nd February 2019. https://main.trai.gov.in/sites/default/files/White_Paper_22022019.pdf. [last accessed on Sept. 24, 2023].
6. Kapoor A, Mishra R, Kumar P. Wideband miniaturized patch radiator for Sub-6 GHz 5G devices. Heliyon. 2021;7(9):1–10. https://doi.org/10.1016/j.heliyon.2021.e07931.
7. Sree GNJ, Nelatur S. Design and experimental verification of fractal based MIMO antenna for lower sub 6-GHz 5G applications. AEU Int J Electron Commun. 2021. https://doi.org/10.1016/j.aeue.2021.153797.
8. Haque MA, et al. Quasi-Yagi antenna design for LTE applications and prediction of gain and directivity using machine learning approaches. Alex Eng J. 2023;80:383–96. https://doi.org/10.1016/j.aej.2023.08.059.
9. Liu G, Zhang C, Chen Z, Chen B. A compact dual band MIMO antenna for 5G/WLAN applications. Int J Microw Wirel Technol. 2022;14(10):1347–52. https://doi.org/10.1017/S175907872100177X.
10. Sharma M, Awasthi YK, Singh H. Design of compact planar triple band-notch monopole antenna for ultra-wideband applications. Wirel Pers Commun. 2017;97:3531–45. https://doi.org/10.1007/s11277-017-4684-3.
11. Haque MA, et al. Machine learning-based technique for resonance and directivity prediction of UMTS LTE band Quasi Yagi antenna. Heliyon. 2023;9(9):1–16. https://doi.org/10.1016/j.heliyon.2023.e19548.
12. Sharma M, Kumar R, Kaur P, Dhasarathan V, Nguyen TK. Design and analysis of on-demand reconfigurable WiMAX/WLAN high isolation 2 × 2 MIMO antenna oriented adjacent/orthogonally for imaging applications in UWB-X band. Int J RF Microw Comput Aided Eng. 2022;31(1):1–15. https://doi.org/10.1002/mmce.22928.
13. Huang B, Li M, Lin W, Zhang J, Zhang G, Wu F. A compact slotted patch hybrid-mode antenna for Sub-6 GHz communication. Int J Antennas Propagat. 2020;2020:1–8. https://doi.org/10.1155/2020/8262361. (**Article ID 8262361**).

14. Paul LC, Hye SA, Rani T, Hossain MI, Karaaslan M, Ghosh P, Saha HK. A compact wrench-shaped patch antenna with a slotted parasitic element and semi-circular ground plane for 5G communication. e-Prime Adv Electr Eng Electron Energy. 2023;6:1–9. https://doi.org/10.1016/j.prime.2023.100334.

15. Azim R, et al. Circular patch planar ultra-wideband antenna for 5G sub-6 GHz wireless communication applications. J Optoelectron Adv Mater. 2021;23(3–4):127–33.

16. Mishra B, Verma R, Yashwanth N, Singh R. A review on microstrip patch antenna parameters of different geometry and bandwidth enhancement techniques. Int J Microw Wirel Technol. 2022;14(5):652–73. https://doi.org/10.1017/S1759078721001148.

17. Desai A, Upadhyaya T, Patel J, Patel R, Palandoken M. Flexible CPW fed transparent antenna for WLAN and sub-6 GHz 5G applications. Microw Opt Technol Lett. 2020;62(12):1–14. https://doi.org/10.1002/mop.32287.

18. Yerlikaya M, Gültekin SS, Uzer D. A novel design of a compact wideband patch antenna for sub-6 GHz fifth-generation mobile systems. Int Adv Res Eng J. 2020;4(2):129–33. https://doi.org/10.35860/iarej.688973.

19. Arya AK, Kim SJ, Kim S. A dual-band antenna for LTE-R and 5G lower frequency operations. Prog Electromagn Res Lett. 2020;88:113–9. https://doi.org/10.2528/PIERL19081502.

20. Nelaturi S. ENGTL based antenna for Wi-Fi and 5G. Analog Integr Circ Sig Process. 2021;107(1):165–70. https://doi.org/10.1007/s10470-020-01766-y.

21. Krishnaveni G, Manimegalai B. Efficient and optimized design of a stacked patch microstrip antenna for next generation network applications. J Ambient Intell Humaniz Comput. 2021;12:4093–9. https://doi.org/10.1007/s12652-020-01788-4.

22. Kapoor A, Mishra R, Kumar P. Compact wideband-printed antenna for sub-6 GHz fifth-generation applications. Int J Smart Sens Intell Syst. 2020;13(1):1–10. https://doi.org/10.21307/ijssis-2020-033.

23. Chowdhury MZB, Islam MT, Rmili H, Hossain I, Mahmud MZ, Samsuzzaman M. A low-profile rectangular slot antenna for sub-6 GHz 5G wireless applications. Int J Commun Syst. 2022;35(17):1–14. https://doi.org/10.1002/dac.5321.

24. Kulkarni J, Sim CYD. Low-profile, compact multi-band monopole antenna for futuristic wireless applications. In: 2020 IEEE international conference on electronics, computing and communication technologies, Bangalore, India; 2020. p. 1–5. https://doi.org/10.1109/CONECCT50063.2020.9198461.

25. Hoque A, Islam MT, Almutairi AF. Low-profile slotted metamaterial antenna based on bi slot microstrip patch for 5G application. Sensor. 2020;20(11):1–18. https://doi.org/10.3390/s20113323.

26. Abdulbari AA, et al. Design compact microstrap patch antenna with T-shaped 5G application. Bull Electr Eng Inform. 2021;10(4):2072–8. https://doi.org/10.11591/eei.v10i4.2935.

27. Balanis CA. Antenna theory: analysis and design. London: Wiley; 2016.

28. Mahmud MZ, Samsuzzaman M, Paul LC, Islam MR, Althuwayb AA, Islam MT. A dielectric resonator based line stripe miniaturized ultra-wideband antenna for fifth-generation applications. Int J Commun Syst. 2021. https://doi.org/10.1002/dac.4740.

29. Singh H, Mittal N, Gupta A, Kumar Y, Woźniak M, Waheed A. Metamaterial integrated folded dipole antenna with low SAR for 4G, 5G and NB-IoT applications. Electronics. 2021;10(21):1–20. https://doi.org/10.3390/electronics10212612.

Discover